ANNUAL REVIEWS

Annual Review of Vision Science

Restoration of Sight with Electronic Retinal Prostheses

Daniel Palanker,[1] James D. Weiland,[2] Boris Rosin,[3] and José-Alain Sahel[3,4]

[1]Department of Ophthalmology, Stanford University, Stanford, California, USA; email: palanker@stanford.edu

[2]Departments of Biomedical Engineering and Ophthalmology & Visual Sciences, University of Michigan, Ann Arbor, Michigan, USA

[3]Department of Ophthalmology, University of Pittsburgh School of Medicine, Pittsburgh, Pennsylvania, USA; email: sahelja@upmc.edu

[4]Institut Hospitalo-Universitaire FOReSIGHT, Paris, France

Annu. Rev. Vis. Sci. 2025. 11:17.1–17.23

The *Annual Review of Vision Science* is online at vision.annualreviews.org

https://doi.org/10.1146/annurev-vision-110323-025244

Keywords

retinal degenerations, blindness, vision restoration, implants, prostheses, rehabilitation

Abstract

Retinal prostheses aim at restoring sight to patients blinded by atrophy of photoreceptors using electrical stimulation of the inner retinal neurons. Bipolar cells can be targeted using subretinal implants, and their responses are then relayed to the central visual pathways via the retinal neural network, preserving many features of natural signal processing. Epiretinal implants stimulate the output retinal layer—ganglion cells—and encode visual information directly in spiking patterns.

Several companies and academic groups have demonstrated that electrical stimulation of the degenerate retina can elicit visual percepts. However, most failed to consistently and safely achieve an acceptable level of performance. Recent clinical trials demonstrated that subretinal photovoltaic arrays in patients visually impaired by age-related macular degeneration can provide letter acuity matching their 100 μm pixel pitch, corresponding to 20/420 acuity. Electronic zoom enabled patients to read smaller fonts. This review describes the concepts, technologies, and clinical outcomes of current systems and provides an outlook into future developments.

1. INTRODUCTION

Retinal degenerative diseases resulting in progressive loss of photoreceptors are among the leading causes of incurable blindness today (Smith et al. 2001). While photoreceptors in retinal degeneration are lost, the inner retinal neurons largely survive (Humayun et al. 1999, Kim et al. 2002, Mazzoni et al. 2008). Retinal prostheses are designed to reintroduce visual information into the neural system by electrical stimulation of the remaining retinal neurons. Several such systems have been evaluated in clinical trials, and more advanced technologies are being developed. This review summarizes various approaches to retinal implants and discusses the challenges and perspectives associated with electronic restoration of sight.

1.1. Encoding of Visual Information in the Retina

The retina, a light-sensitive part of the central nervous system, consists of three neural layers—photoreceptors, the inner nuclear layer, and the ganglion cell layer—separated by two plexiform layers, where cells' axons and dendrites connect (**Figure 1*a***). The human retina contains about 120 million photoreceptors. Cones dominate the central regions of the visual field and are responsible for day vision. Rods dominate the periphery and mediate night vision. Primates and humans

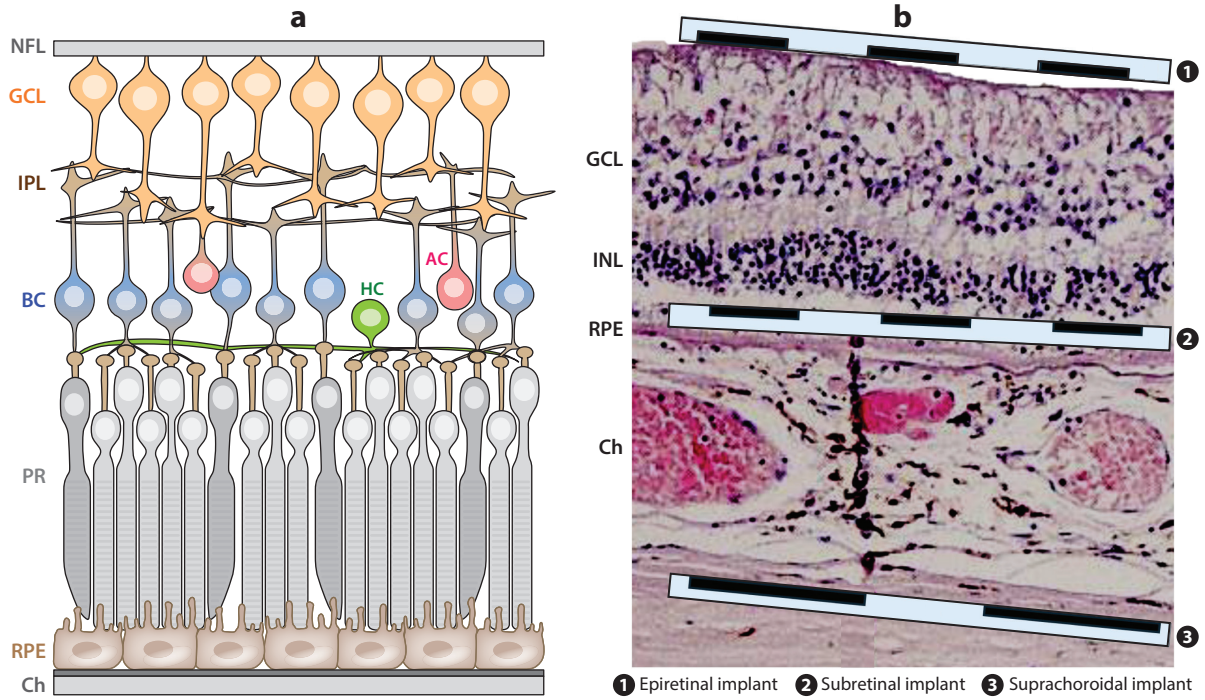

Figure 1

Retina and implant placement. (*a*) Simplified diagram of the retina. Signals from PRs, which are located at the back of the eye and contact the RPE, are relayed to BCs, which are regulated by HCs. Axons of BCs are wired to the dendrites of GCs in the IPL, which is regulated by ACs. Axons of GCs form the NFL, which relays visual signals to the brain. (*b*) Histological cross-section of a degenerate human retina with diagrammatic representations of an epiretinal implant (Smith et al. 2001), subretinal implant (Mazzoni et al. 2008), and a suprachoroidal implant (Humayun et al. 1999). Abbreviations: AC, amacrine cell; BC, bipolar cell; Ch, choroid; GC, ganglion cell; GCL, ganglion cell layer; HC, horizontal cell; INL, inner nuclear layer; IPL, inner plexiform layer; NFL, nerve fiber layer; PR, photoreceptor; RPE, retinal pigment epithelium.

have three distinct cone subtypes in their eyes, called S, M, and L cones, with peak sensitivity in the short (blue), medium (green), and long (yellow-red) wavelengths (Wandell 1995).

Photoreceptors relay visual information to neurons in the inner nuclear layer of the retina, which is composed of about 10 million cells in a human eye, where two types of horizontal cells, about 12 types of bipolar cells, and as many as 30 types of amacrine cells (Masland 2001, Wassle 2004) process visual signals. Like photoreceptors, retinal interneurons are primarily nonspiking, even though some amacrine cells can produce action potentials (Greschner et al. 2014). Retinal interneurons pass on visual information to more than 20 distinct classes of retinal ganglion cells (RGCs) (about one million in a human eye) that generate action potentials, which propagate via the optic nerve to the brain.

Bipolar cells relay visual information from photoreceptors to ganglion cells. Horizontal cells modulate the synapses between photoreceptors and bipolar cells and are involved in contrast adaptation and in the antagonistic center-surround effect. Amacrine cells regulate the synapses between bipolar and ganglion cells, performing multiple complex computations, including the antagonistic center-surround effect, motion selectivity, temporal modulation, and many other functions in the retina (Briggman et al. 2011).

Bipolar and ganglion cells that respond to increments of light over the center of their receptive fields are called ON cells, while those that respond to light decrements are called OFF cells. In the primate retina, midget ganglion cells having small receptive fields are thought to be responsible for high acuity vision, and the parasol ganglion cells with large receptive fields project to areas of the brain thought to encode motion (Britten et al. 1992, Merigan & Maunsell 1993, Salzman et al. 1990). Each of the two dozen different types of RGCs (representing ON and OFF pathways, different colors, various resolution and contrast sensitivity levels, temporal aspects of the response, etc.) covers the entire retina, forming overlapping mosaics. The brain decodes the input image from their population response.

Spatial resolution of normal vision is limited by cone spacing in the central macula (i.e., sampling limit) and by the diffraction limit of the human eye, both of which can reach approximately 3 μm on the retina. Normal vision is defined as the ability to recognize optotypes subtended to a visual angle of 5 minutes of arc, which corresponds to lines separated by 1 minute of arc, which in turn corresponds to 5 μm per line on the retina or to angular resolution of 30 cycles per degree. Visual acuity is often expressed in fractions, such as 20/20 for normal vision in the United States, or 6/6 in metric units. Legal blindness in the United States corresponds to acuity 10 times lower than normal (i.e., 20/200 or a visual field smaller than 20°), while the World Health Organization sets the limit at 20/400 (Dandona & Dandona 2006). Therefore, pixels of 5 μm on retinal implants are required to represent patterns at the resolution of normal vision (i.e., 20/20), and pixels of 50 μm are required for acuity of 20/200. Another common measure of acuity is the logarithm of the minimum angle of resolution, LogMAR. Resolution of 1 minute of visual angle (i.e., normal vision) corresponds to LogMAR 0 (since log 1 = 0), resolution of 10 minutes of visual angle corresponds to LogMAR of 1, and so on. Another commonly used criterion for legal blindness is visual field restriction below 20°.

1.2. Retinal Degeneration and Its Effects on the Visual System

The leading cause of incurable blindness in the developed world today is a broad category of diseases known as retinal degeneration (Haim 2002, Smith et al. 2001). In these conditions, photoreceptors gradually disappear, leading to loss of sight. However, neurons in the inner nuclear and ganglion cell layers mostly survive and can be stimulated electrically, making them target candidates for retinal prosthetics (**Figure 1*b***).

Age-related macular degeneration (AMD) is a leading cause of untreatable vision loss, affecting over 8.7% of the population worldwide (Wong et al. 2014). Advanced forms of AMD (i.e., neovascular and geographic atrophy) are associated with severe visual impairment, and their prevalence dramatically increases with age, from 1.5% in the US population older than 40 years to more than 15% in the US population older than 80 years (EDPRG 2004). Geographic atrophy, which affects approximately 8 million people worldwide (Rudnicka et al. 2012), is associated with a gradual loss of photoreceptors in the macula, which encompasses the center of the visual field and is responsible for high-resolution vision. This can severely impair visual functions, such as reading and face recognition. Low-resolution peripheral vision is retained in this condition, necessitating the use of eccentric fixation. Therefore, any treatment strategy to provide functional central vision should aim not to jeopardize the surrounding healthy retina.

Retinitis pigmentosa (RP) is a broad class of a variety of genetic disorders that typically present in patients during their third or fourth decade of life, and it has an incidence rate of approximately 1:4,000 (Haim 2002). Statistically, by the age of 50 years, approximately 50% of patients with RP can be diagnosed as legally blind, although marked variability exists between different inheritance modes and subtypes (Berson 2007). This inherited disease typically begins with loss of rod photoreceptors in the periphery, followed by loss of cone photoreceptors in the central retina. As the disease progresses, visual field restriction progresses to tunnel vision, with some bare light perception in the periphery. Eventually, central light sensitivity can disappear as well. The majority of RP patients retain some degree of sight (Grover et al. 1999); thus, only the patients with acuity significantly lower than that provided by retinal implants can be considered candidates for prosthetic vision.

To restore functional vision in patients blinded by RP, retinal implants should provide a sufficiently large field of view for comfortable orientation and ambulation, ideally exceeding 20°. In AMD patients, however, a central scotoma rarely exceeds 10–15° of the visual field, so ambulation is not a problem. Therefore, in AMD patients with geographic atrophy, the implant should cover about 10° in the middle of the scotoma and avoid damage to the adjacent healthy retina.

While retinal degenerations leave the inner nuclear layer and RGCs relatively intact for an extended period of time (Humayun et al. 1999), significant changes in retinal organization can take place at the end stages of the disease, when the vast majority of photoreceptors are lost (Jones & Marc 2005, Marc & Jones 2003, Marc et al. 2003). These changes are broadly called retinal remodeling. During this process, amacrine and bipolar cells can migrate either to the outer retina or to the ganglion cell layer. While all neurons appear to retain their normal basic molecular signatures, new synaptic connections are abundant. In the final stages of retinal remodeling, neuronal death can significantly deplete the inner nuclear and ganglion cell layers, with glial cells partially filling the space left by deceased neurons (Marc & Jones 2003, Marc et al. 2003). Spontaneous firing patterns of RGCs change considerably with degeneration (Margolis et al. 2008, Menzler & Zeck 2011, Sekirnjak et al. 2011), including asynchronous rhythmic activation at 7–10 Hz in the *rd1* mouse (Menzler & Zeck 2011) and periodic bursting in the *rd10* mouse (Cho et al. 2016).

AMD patients are less likely to suffer from extensive retinal remodeling than RP patients. This is since (*a*) the onset of the disease is much later in life and hence its duration is shorter (a few years or decades in patients with AMD versus several decades in patients affected with an inherited disease such as RP), and (*b*) the peripheral retina is preserved, which helps in maintaining more physiological neural activity in the center via lateral connectivity in the retinal network. However, even in focal retinal degeneration, the RGC spiking rate may increase significantly (Tochitsky et al. 2014).

1.3. Electrical Stimulation of Neurons

Application of electric field to tissue leads to polarization of cells: Since the cell membrane is highly resistive and its cytoplasm is very conductive, charges redistribute along the cell membrane, and the cytoplasm rapidly (μs range) becomes equipotential (Boinagrov et al. 2010). As a result, the transmembrane voltage increases (i.e., the membrane becomes hyperpolarized) on the side of the cell facing the anode and decreases (i.e., the membrane becomes depolarized) on the opposite side. On the depolarized side of the membrane, the voltage-gated cation channels open, increasing the influx of positive ions (Na^+ in ganglion cells and Ca^{++} in bipolar cells), resulting in cellular depolarization as a whole. When the membrane potential exceeds a certain threshold, the action potential occurs in spiking neurons (e.g., RGCs). In contrast, photoreceptor cells respond by increasing the neurotransmitter release rate in axonal terminals (e.g., retinal bipolar cells). Typically, at least 10 mV across a cell soma is required to elicit a response (Boinagrov et al. 2010).

If the action potential occurs during the stimulation pulse, the threshold current does not depend on pulse duration. This regime of stimulation is called rheobase. When the stimulus ends before the action potential is generated, the influx of sodium ions during the stimulus may still be sufficient to put the neuron on the path of generating the action potential. The shorter the pulse, the stronger the stimulus needs to be to allow sufficient charge influx to exceed the stimulation threshold. This mechanism defines the rising part of the strength-duration dependence of the stimulation threshold with decreasing pulse duration (Boinagrov et al. 2010). Pulse duration at which the threshold is twice the rheobase is called chronaxie. Since the kinetics of different ion channels can vary significantly, chronaxie varies between different cell types, providing an opportunity for their selective activation.

Since the distribution of ion channels over neurons is rarely isotropic, the orientation of the electric field significantly affects the stimulation threshold. It is lower when the side of the cell with the highest concentration of the responding ion channels is depolarized. Therefore, optimal pulse polarity (i.e., anodic or cathodic) depends on the location of the stimulating electrode: For epiretinal stimulation of RGCs, cathodic pulses have lower stimulation thresholds (Boinagrov et al. 2014, Fried et al. 2006, Jensen et al. 2005) due to the higher concentration of Na channels over the region of RGCs facing the inner limiting membrane, near the axonal hillock (Fried et al. 2006). For subretinal stimulation of RGCs, anodic pulses have lower stimulation thresholds for the same reason (Boinagrov et al. 2014, Jensen & Rizzo 2006). Similarly, for subretinal stimulation of bipolar cells, anodic pulses have lower thresholds (Boinagrov et al. 2014) because bipolar cells have higher concentrations of Ca ion channels in their axonal terminals (Werginz et al. 2015). For small electrodes, proximity to the target neuron is another factor that significantly affects stimulation thresholds, since in this case the electric field rapidly decreases with distance. Yet another factor is the optimal pulse duration: Na channels in RGCs respond faster to membrane depolarization than Ca influx in bipolar cells. Therefore, chronaxie of RGCs is shorter (< 1 ms) than that of bipolar cells (> 2 ms), providing an opportunity for selective stimulation of the desired cell types (Boinagrov et al. 2014). A combination of good electrode placement and proper choice of stimulation pulse parameters can help achieve selective activation of the various neural layers (Boinagrov et al. 2014).

2. APPROACHES TO RETINAL PROSTHETICS

2.1. Anatomical Placement of Stimulating Electrodes

Depending on their location in the patient's eye, retinal implants fall into one of three categories: epiretinal, subretinal, or suprachoroidal (**Figure 1*b***). In the epiretinal approach, prostheses target primarily RGCs using electrodes placed above the nerve fiber layer (Ahuja et al. 2011,

Humayun et al. 2012). Since the action potential is a binary response, modulating the stimulus amplitude above the threshold does not affect the amplitude of the resulting spike, and hence the natural modulation strategy for RGCs is by stimulation frequency. Epiretinal devices are less dependent on the health of the inner retina and can operate if the RGCs survive. However, an abnormally high spontaneous firing rate of ganglion cells, frequently observed in animal models of retinal degeneration, is a problem since it impedes the ability of the implant to encode a desired sequence of spikes or diminishes the corresponding perception.

In the subretinal approach, arrays of electrodes located between the inner nuclear layer and the pigment epithelium replace the degenerated photoreceptors and target the surviving second-order neurons, bipolar cells (Lorach et al. 2015, Zrenner et al. 2011) (**Figure 1*b***). Subretinal implants deliver visual information to nonspiking inner retinal neurons, and stronger stimuli are encoded with higher amplitude or longer duration pulses. Output signals from bipolar cells are then transmitted via the retinal neural network and converted into action potential trains in RGCs. This approach allows for the maintenance of some of the signal processing properties of the retina, so the spiking patterns elicited by RGCs resemble those arising under normal physiological conditions. However, adaptive changes in the retinal network during degeneration may significantly impact signal processing and limit our ability to encode visual information.

Implanting a subretinal device involves the creation of a local retinal detachment and a small retinal incision, through which the device is placed into the subretinal space, after which the retina is reattached (Palanker et al. 2020). Excessively traumatic implantations can lead to fibrosis, atrophy, and scarring. In the case of wired subretinal implants, large areas of the retina need to be detached during implantation, presenting a significant challenge with fragile diseased retinas (Daschner et al. 2018). Explanting a subretinal device is significantly more difficult than explanting an epiretinal device, although it has been done with Alpha-IMS implants and with photovoltaic subretinal devices (Bhuckory et al. 2025).

In the suprachoroidal approach, the implant is placed below the choroid into the sclera (**Figure 1*b***). While this approach has been deemed to be surgically less risky than both epi- and subretinal prostheses (Ayton et al. 2014, Fujikado et al. 2011), the larger distances between the stimulating electrodes and retinal neurons greatly restricts attainable spatial resolution. Therefore, such implants have large ($\sim$ mm) electrodes and are designed to help restore low-resolution peripheral vision, primarily for ambulation.

2.2. Delivery of Information and Power to the Implant

Since direct connection of an implant to external electronics via transcutaneous wire often leads to infections and severe scarring (Knutson et al. 2002), transmission of information and power to the implant should be wireless, using either radiofrequency (RF) coils or light. The transmitting and receiving coils in implanted systems are typically weakly coupled (Wang et al. 2005), with the coupling coefficient k in the range of 0.08 to 0.24, hence involving significant power loss. Quality factor Q of the transmitter and receiver increases with frequency; however, RF absorption in tissue increases exponentially beyond a few megahertz (Osepchuck 1983), limiting the range of useful frequencies to below a few megahertz. Another option is transmission of power via an RF link, but serial telemetry of data, via the much faster optical link, was implemented in the Intelligent Retinal Implant System (IRIS) II (Pixium Vision, Paris, France) (Hornig et al. 2017).

Since visual information transmitted from the camera to the implant via serial telemetry does not depend on eye movements, this approach creates perceptual problems: Because stimulation patterns in such implants do not translate with the moving eye, the brain interprets this lack of retinal shift as motion of the object. Similar effects have been reported with cortical visual

prostheses (Naumann 2012). To avoid this phenomenon, patients are asked to keep their direction of gaze steady and scan the visual field with their heads—a very unnatural paradigm. These limitations can be alleviated by incorporating an eye tracking system, which electronically shifts the image delivered to the implant according to the direction of gaze (Caspi et al. 2018).

A few designs are based on power transmission via inductive coupling and visual information through natural eye optics (Ha et al. 2016, Loudin et al. 2007, Woodburn et al. 2002, Zrenner et al. 2011). One such system was the Alpha-IMS/AMS (Retina Implant AG, Reutlingen, Germany). Each pixel in such subretinal implants had a light sensor, amplifier, and stimulating electrode, which together converted incident images into electrical stimulation patterns. A subdermal power-receiving coil was placed behind the ear, similar to cochlear implants, with its output routed to the subretinal implant via a transscleral cable (Stingl et al. 2017).

The third category of retinal implants receives both data and power by light via the natural optics of the eye (Ghezzi et al. 2013, Mathieson et al. 2012). These implants directly convert incident light into electric currents to stimulate the nearby neurons. Using an array of photodiodes as a subretinal implant was first proposed in the 1990s (Chow et al. 2004). In that design, the photovoltaic pixels in the implant were expected to convert ambient illumination into stimulating currents. However, ambient light on the retina is much too dim for photovoltaic stimulation (Palanker et al. 2005a). In addition, photovoltaic conversion of continuous illumination cannot provide charge-balanced current pulses, which are required to avoid irreversible electrochemical reactions. A revised concept of a photovoltaic subretinal implant powered by intense pulsed light projected from augmented reality glasses was proposed in 2005 (Palanker et al. 2005a), first implemented in 2007 (Loudin et al. 2007), and actively developed since then (Lorach et al. 2015, Mathieson et al. 2012). To avoid photophobic and phototoxic effects of bright illumination, photodiode-based systems use near-infrared (850–915 nm) wavelengths, which are invisible to the remaining photoreceptors.

2.3. Safety Considerations

For both RF- and optically powered implants, tissue heating resulting from absorption of electromagnetic radiation and energy dissipation in the implanted electronics must be kept within acceptable safety limits. International Organization for Standardization norm 14708-1 article 17.2 specifies that temperature rise in chronic operation should not exceed 2°C (ISO 2014).

Electrical stimulation of neural tissue has the potential to cause irreversible cellular damage (McCreery et al. 1990). One mechanism of damage is electroporation: Strong electric fields can produce sufficiently high transmembrane voltage (~ 1 V) to make penetration of polar molecules of water into the hydrophobic lipid bilayer energetically favorable, which leads to the formation of nanometer-scale pores in the cell membrane (Neumann 1992). The damage threshold current density j scales inversely with the square root of pulse duration ($j \sim t^{-0.5}$) (Butterwick et al. 2007). Since neural stimulation threshold scales as $1/t$ on the short end of pulse duration and is flat (rheobase) on the long end, the ratio of the electroporation threshold to neural stimulation threshold decreases toward shorter and longer pulses as $t^{0.5}$ or $t^{-0.5}$, respectively, with its maximum near chronaxie. With large electrodes, retinal stimulation thresholds are approximately two orders of magnitude below the electroporation thresholds (Butterwick et al. 2007), leaving a sufficiently wide window for safe stimulation of the retina.

In addition to cellular hyperthermia and electroporation, cellular damage can also be caused by the leaching of toxic electrode materials into the medium or by local changes in pH. Neural stimulation electrodes have been extensively studied in recent years, and a large literature on the topic is available (Cogan 2008, Merrill et al. 2005, Robblee & Rose 1990). Electrochemical safety limits

vary with electrode materials and with mechanisms of charge injection, which are either capacitive or faradaic (Cogan 2008). For both mechanisms, stimulation pulses need to be charge balanced and within the safe limits of electrode potential to avoid irreversible oxidation or reduction of the electrode material and other irreversible electrochemical reactions in the medium, such as water electrolysis and metal dissolution (Cogan 2008, Merrill et al. 2005, Robblee & Rose 1990).

3. MAIN CLINICAL TRIALS

Clinical studies have been conducted with multiple epiretinal, subretinal, and suprachoroidal implants. Several have received regulatory approval, although none that received US Food and Drug Administration (FDA) approval and/or EU approval (the CE mark) succeeded as commercial medical devices. In this section, we summarize the status of retinal prostheses tested in humans (**Table 1**). Some of these underwent only small-scale feasibility tests, while others completed the clinical trials required for regulatory approval. Below, we group the retinal implants by their location: epiretinal prostheses, anchored to the inner surface of retina; subretinal prostheses, embedded between the retina and the retinal pigment epithelium (RPE) or the choroid; and suprachoroidal prostheses, implanted between the sclera and the choroid.

3.1. Epiretinal Prostheses

Two generations of devices, Argus I and Argus II, were developed by Second Sight Medical Products (SSMP). Argus I was approved as an investigational device by the FDA, which allowed a US clinical trial to be conducted. Argus I was a modified 16-channel cochlear implant, having a 4×4 array of platinum electrodes for epiretinal placement (Humayun et al. 2003). Argus I was used to demonstrate chronic safety and feasibility of epiretinal stimulation. The implantable system's size required placement of the stimulator behind the ear with a cable running into the orbit. The Argus II retinal implant (Humayun et al. 2012) was designed as a novel device, with a new stimulator having 60 individual channels. Argus II was evaluated in a multicenter clinical trial, which resulted in CE marking in 2011 and FDA market approval in 2013. The Argus I and II systems include a miniature camera mounted on a pair of glasses, a wearable external video processing unit, a pair of external and implanted coils for data and power transmission, and an electrode array mounted on the retina using a custom tack (**Figure 2**).

Argus I was implanted in 6 subjects with end-stage RP between 2002 and 2004. All patients reported light perception when the device was activated, including patients with several years of no light perception. The safety of the device was confirmed in every patient, but 1 subject elected to have the device removed due to an unrelated health problem. Each patient had the ability to perform simple visual tasks, such as detecting, counting, and discriminating objects (Yanai et al. 2007). One Argus I subject was tested 10 years after implantation and reported phosphene perception (Yue et al. 2015).

Between the years 2007 and 2009, a total of 30 subjects (29 with RP and 1 with choroideremia) received the Argus II implant in the United States and Europe (Ho et al. 2015). All patients reported light detection and performed visual spatial and motion tasks after a short period of training. With the system on, more than 90% of the subjects performed a spatial-motor task (i.e., locate and touch a white square on a black computer screen) with greater accuracy and repeatability than with the system off (Ahuja et al. 2011). The best reported visual acuity improved from 20/3244 with Argus I to 20/1262 with Argus II. Most patients demonstrated the ability to identify large high-contrast letters with the device on, as opposed to when it was off. However, head scanning was always required, and the time spent on this task was relatively long (i.e., tens of seconds) (daCruz et al. 2010). A significant problem with Argus II is the stimulation of axons passing near

Table 1 Various implants tested

Device (company)	Device type	Main findings	Clinical studies and device status
Argus I (SSMP)	Epiretinal	Large object detection, social connection, safety of long-term implantation and stimulation	6 patients implanted from 2002–2004, not a commercial product
Argus II (SSMP)	Epiretinal	Visual acuity up to 20/1260, large object detection, letter discrimination, social connection, improved mobility, longevity (10-year lifetime demonstrated)	30 subjects, multisite trial, FDA approval, CE mark, Argus II no longer sold, company closed in 2019
IRIS II (Pixium Vision)	Epiretinal	Object localization, motion detection, object recognition, device failure noted	10 patients implanted, CE mark, not commercialized, in part due to poor robustness
IMIE 256 (Golden Eye Bionics)	Epiretinal	Visual acuity up to 20/800, motion detection, improved mobility	Completed 3-month study of 5 patients, devices explanted
NR600 (Nanoretina)	Epiretinal, penetrating	Light perception, stable position up to 2 years, object localization	9 patients implanted in a feasibility study, company closed in 2023
ASR (Optobionics)	Subretinal	Light sensitivity, neurotrophic effect (improved central vision from implant in periphery)	30 patients implanted in multicenter trial, the ASR never received regulatory approval, company closed
Alpha-IMS and Alpha-AMS (Retina Implant AG)	Subretinal	Visual acuity up to 20/546 (in 2 patients), letter reading, object discrimination, motion detection, activities of daily living improvement	IMS: first device, implanted in 9 patients AMS: improved device, CE mark, 39 patients implanted, company closed in 2019
PRIMA (Pixium Vision, now Science Corp.)	Subretinal	Prosthetic visual acuity (Landolt C) of 20/438 to 20/565, integration of natural peripheral and prosthetic central vision	Feasibility clinical trial with 5 patients (2018–2023)
		With no zoom, average letter acuity of 20/420, and with zoom, acuity up to 20/63, mean improvement of acuity versus baseline of 24 ETDRS letters (4.8 lines)	Phase III pivotal trial with 38 patients in 5 countries, 12-month follow-up completed in January 2024, Pixium Vision acquired by Science Corp. in 2024
Bionic Eye System (Bionic Vision Technologies)	Suprachoroidal	Stable condition of retina and position at up to 10 years (3 patients) and 5 years (4 patients), perception of light, improvements in mobility and functional vision	44-channel devices tested in 4 subjects, functional at 2.7 years post-implant, FDA Breakthrough Device Designation, no regulatory approval at the time of this review
STS (Nidek)	Suprachoroidal	Object localization	Report on 3 patients with 6-month implants, not commercialized

Abbreviations: ASR, Artificial Silicon Retina; FDA, US Food and Drug Administration; IMIE, Intelligent Micro Implant Eye; IRIS, Intelligent Retinal Implant System; SSMP, Second Sight Medical Products; STS, suprachoroidal-transretinal stimulation.

the electrodes from remote RGCs. Percepts induced by axonal stimulation have arcuate rather than punctate shapes, severely distorting the retinotopic map of the visual field (Behrend et al. 2011, Nanduri et al. 2012).

After FDA approval of Argus II, around 400 devices were implanted worldwide. Further clinical studies demonstrated a reduction in adverse events for implantations performed after FDA approval, likely due to experience gained in surgical procedures during the clinical trial

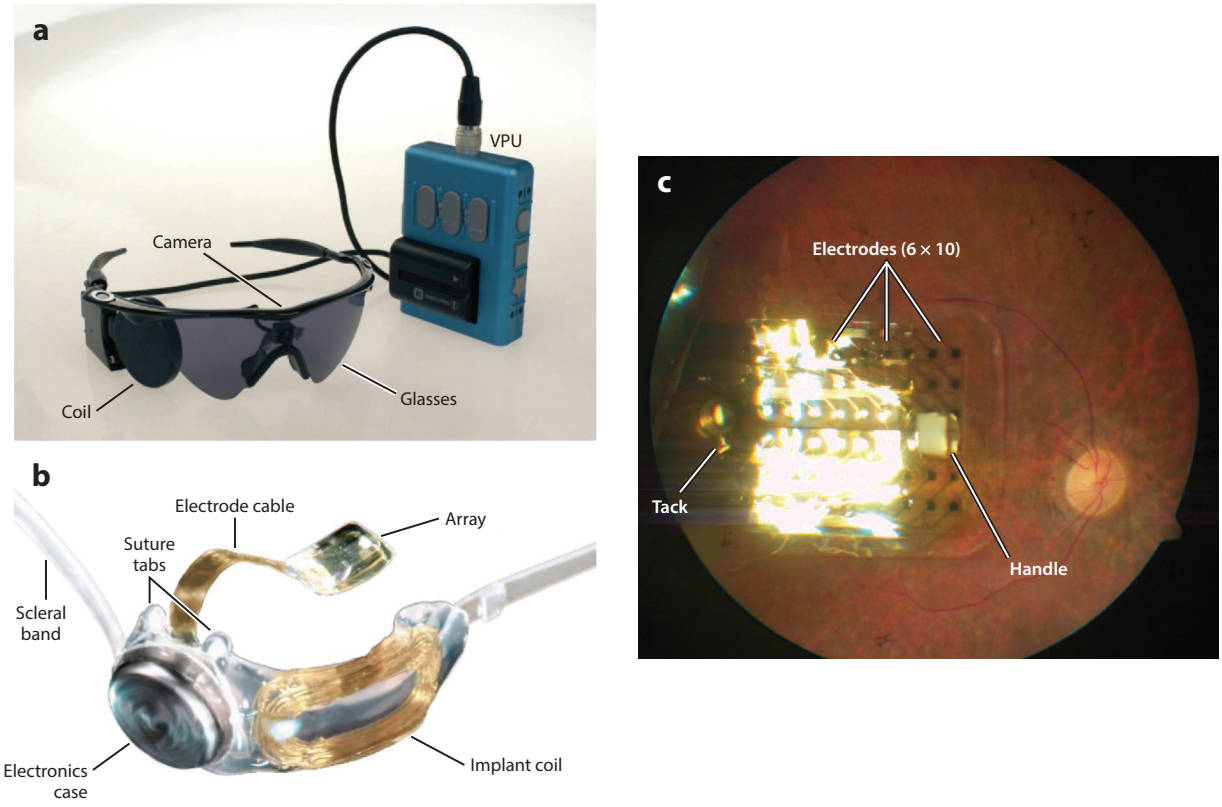

Figure 2

The Argus II epiretinal implant. (*a*) Photograph of the external portion of the Argus II prosthesis system, including a glasses-mounted video camera, radiofrequency (RF) coil, and video processing unit (VPU) with a rechargeable battery. (*b*) Photograph of the implantable portion of the Argus II prosthesis system, including the 6 × 10 electrode array, electronics case, and the implant RF coil. (*c*) Fundus photograph of an Argus II array implanted in the macular region. A retinal tack secures the electrode array to the sclera. The surgeon uses the white handle to position the device in the eye. Figure adapted from Humayun et al. (2012).

(Delyfer et al. 2021). In this same group of subjects, positive impacts of the Argus II system on functional vision and well-being were demonstrated for more than 70% of subjects in the Functional Low-Vision Observer Rated Assessment (Geruschat et al. 2016). Finding doorways and detecting obstacles were notably improved. A study of 20 patients was conducted to document the progression of epiretinal membranes commonly observed in Argus II patients (Rizzo et al. 2019). Optical coherence tomography revealed the development of a fibrosis-like hyperreflective tissue at the interface between the array and retina in 10 eyes (50%). In 9 of 10 patients (90%), fibrosis evolved and progressed to retinoschisis. Despite the development of fibrosis and schisis, there was no deterioration in the patients' visual performance as evaluated prospectively with visual function tests (i.e., square localization and direction of motion).

In 2020, SSMP drastically reduced its operation due to lack of sufficient clinical acceptance of Argus II. Even though it provided some benefits, such as help with navigation in specific circumstances and increased social engagement, real-life navigation did not improve as patients remained severely visually impaired. The limited benefits resulted in poor adoption by patients.

The IRIS II was implanted in 10 patients between 2016 and 2017 (NCT 02670980). Like Argus II, it had an external camera and video processing system (Hornig et al. 2017). The implantable electronic module was positioned in the orbit and sutured to the side of the eye. A cable connected to an array of 150 electrodes entered the eye and was tacked to the retina. IRIS II included a neuromorphic image sensor that responded to changes in illumination, and a video processor was used to highlight important parts of an image. Results from the IRIS II clinical trial showed better object localization, direction of motion, and picture recognition (Hornig et al. 2017). Later reports noted lack of robustness, with multiple device failures within 1 year. Pixium abandoned the IRIS II approach to focus on the PRIMA subretinal implant.

A more recent epiretinal implant, NR600 (Nanoretina), was tested in a small clinical feasibility study of 9 patients (Yanovitch et al. 2022). Its entire electronics module, including camera, stimulator circuit, and hermetic packaging, was miniaturized into a device that could be implanted inside the eye. Power was provided wirelessly by an external infrared light source. An array of 600 individual electrodes (20 × 30) spaced 100 μm apart was designed to penetrate the retina. While the bench testing of the device is well described and the device worked as designed, the clinical study was not described in enough detail to assess functional vision provided by the device. Patients could see light when the implant was activated, but visual function was not reported in detail. Grating acuity was reported in only 1 patient, and this result was far below the theoretical visual acuity based on the device's electrode spacing. Nanoretina ceased operation in 2023.

The 256-channel Intelligent Micro Implant Eye (IMIE 256, Golden Eye Bionics) was recently tested clinically (Xu et al. 2021). The IMIE 256 is similar to Argus II in its architecture: Using RF coils, an external system communicates with an implanted stimulator sutured to the side of the eye. A retinal electrode array with 256 channels is tacked to the epiretinal surface. Five patients were implanted with the IMIE 256 for a semichronic study, with planned explantation after 90 days. Each experiment showed better performance with the device on versus off. Grating acuity of 20/800 was estimated in all 5 subjects, but the number of trials was small (less than 5). Patients also performed better than chance with object localization, line following, and door detection, but again the number of trials reported was too small to make a definitive statement about system efficacy. Devices were explanted with no adverse events related to surgical procedures.

3.2. Subretinal Prostheses

A subretinal prosthesis is placed between the RPE and the degenerate retina, stimulating the first layer of inner retinal neurons, bipolar cells. In all three subretinal prostheses tested in humans, image detection was done using microphotodiodes integrated into the pixels of a subretinal chip. In other words, the camera was inside the eye, which is an important feature that properly couples eye movement with visual perception. With this in common, there are many differences in subretinal devices, as described below.

3.2.1. The Artificial Silicon Retina. The Artificial Silicon Retina (ASR) developed by Optobionics was the first retinal implant to be evaluated in an FDA-approved clinical trial. The ASR is a silicon-based chip, 2 mm in diameter and 25 μm thick. This device contains approximately 5,000 microphotodiodes of 25 μm in size, each coupled to a 9 × 9 μm iridium oxide electrode, and functions passively without external power and wires (Chow et al. 2004). In 2000–2001, the ASR was implanted in the mid-periphery of the retina (close to arcades) and tested in more than 10 RP patients, 6 of whom have been followed up to > 7 years (Chow et al. 2010). Although safety and improvement in visual function have been observed in most of the patients, these improvements were found in the central field, far from the implant site (Chow et al. 2004, 2010). They have been attributed to the neurotrophic effects of the implant that rescued or preserved the damaged cells in

the retina. Under ambient retinal illumination, the ASR's microphotodiodes could produce < 1 nA of current, whereas activation thresholds of retinal neurons are typically in μA range (Palanker et al. 2005b). Moreover, due to the capacitive coupling of electrodes to electrolyte, it cannot generate continuous current under continuous illumination. Subsequent subretinal implants address this limitation by using intensified and pulsed infrared light or electronic amplifiers to generate sufficient current.

3.2.2. The ALPHA-IMS implant. The Alpha-IMS (Retina Implant AG, Reutlingen, Germany) addressed the low intensity of natural light in the eye by including externally powered amplifiers in each pixel (**Figure 3**). In the investigational device, power was supplied via a percutaneous cable with a connector positioned behind the ear. The percutaneous cable was replaced by a subdermal power module for wireless transmission (Wilke et al. 2011) in the commercial device. The microphotodiode array chip consists of about 1600 pixels of 70 μm in size, containing photodiodes and differential amplifiers, coupled to 40 × 40 μm electrodes coated with titanium nitride. The size of the chip is roughly 3 × 3 mm, covering a visual angle of about 10° × 10°.

One of the Alpha-IMS trials included 29 patients with hereditary eye disease, 25 with RP, and 4 with cone–rod dystrophy (Stingl et al. 2015). The implant was placed under the central macula, with the flat power cable running under the retina to a transscleral slit near the equator. Within 10 months of postoperative observation, 21 participants reached the primary experimental end point, of which 13 showed significant restoration of visual function used in daily life. The report further showed that 3 patients could read letters, in which the visual angle was subtended to up to 10°. The best reported visual acuity with Landolt C optotypes was 20/546, roughly half the theoretical limit for 70 μm pitch of electrodes (20/280). The study was curtailed by device failure a few months post implantation due to nonhermetic packaging, with chip corrosion leading to malfunction of the electronics (Daschner et al. 2018). The next-generation implant, Alpha-AMS, improved the materials and fabrication processes to overcome these durability issues. Small changes were made to the subretinal chip design as well (Stingl et al. 2017). A clinical study with 15 patients reported visual function results similar to those found in earlier studies with Alpha-IMS (Stingl et al. 2017), which is not surprising since the electrode array geometry did not change significantly. However, these implants still failed over time (albeit slower), and Retina Implant AG ceased operations in 2019.

3.2.3. PRIMA. The PRIMA neurostimulation system (Science Corp., formerly Pixium Vision) was developed to provide central vision in geographic atrophy of AMD patients by replacing lost photoreceptors with a subretinal photovoltaic array, which converts light into electric pulses to stimulate second-order retinal neurons (i.e., bipolar cells) (Lorach et al. 2015). Because (*a*) photovoltaic cells require light brighter than ambient for stimulation and (*b*) current should be pulsed to preserve the charge balance, images captured by a camera are projected from augmented reality glasses onto the implant using pulsed light (**Figure 4**). To avoid any confounding effect of this intense light on photoreceptors outside of the geographic atrophy, its wavelength is beyond the visible part of the spectrum, in the near-infrared range (880 nm). The 2 × 2 mm PRIMA implant is 30 μm thick and composed of 100 μm pixels. A pocket computer provides image processing, including adaptation to ambient illumination, contrast enhancement, and zoom (magnification 1x, 2x, 4x, and 8x), for prosthetic vision, while leaving peripheral natural vision unaffected. Since the photovoltaic implant is powered by light, it has no wires, greatly simplifying surgical procedures.

Following extensive preclinical testing (Arens-Arad et al. 2020; Ho et al. 2018a,b; Lorach et al. 2015), a clinical feasibility trial of the PRIMA system was conducted to assess its safety and efficacy in AMD patients suffering from profound central vision impairment due to geographic atrophy. Five patients who received implants in 2018 at a single center in Paris, France, demonstrated

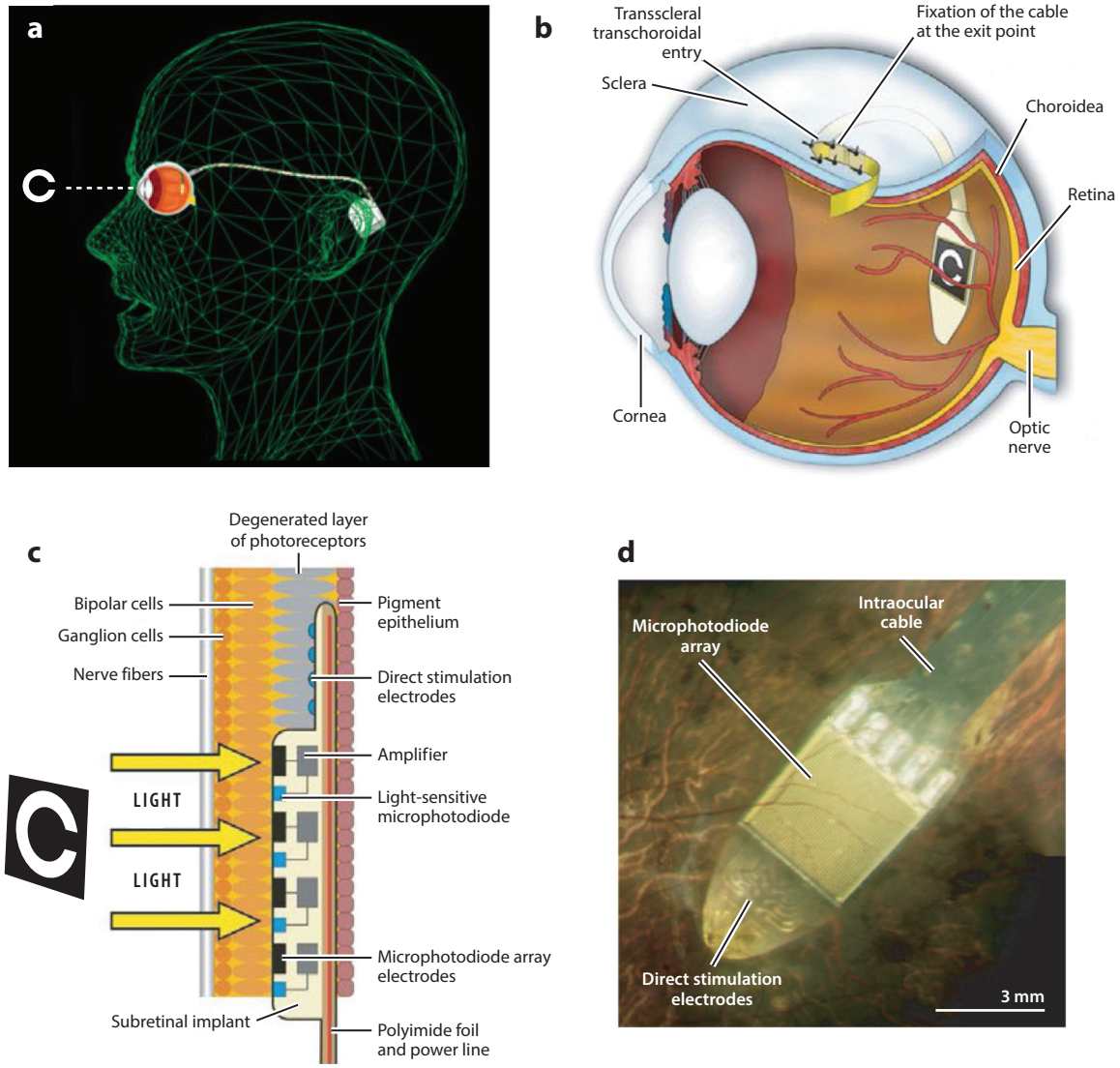

Figure 3

The Alpha-IMS subretinal implant. (*a*) The cable from the subretinal chip leads through the sclera, under the temporal muscle to the radiofrequency receiver behind the ear. (*b*) Implant under the transparent retina, with the power cable exiting the eye 3 mm behind the limbus. (*c*) Subretinal camera with photodiodes, amplifiers, and electrodes in relation to retinal neurons and pigment epithelium. (*d*) View of the tip of the subretinal implant at the posterior pole through a patient's pupil. Scale bar: 3 mm, corresponding to 10° visual angle. Figure adapted from Zrenner et al. (2011) (CC BY 4.0).

preservation of their peripheral vision. Prosthetic central vision enabled patients to reliably recognize letters and sequences of letters, with acuity closely matching the maximum resolution allowed by the 100 μm pixels, corresponding to 20/420 (Palanker et al. 2020). Remarkably, patients can perceive prosthetic vision simultaneously with residual peripheral natural vision (Palanker et al. 2022). Using zoom functionality, visual acuity improved up to 8 ETDRS lines (up to 20/63) compared to baseline, demonstrating clinically meaningful benefits of prosthetic central vision in the former scotoma (Muqit et al. 2024). Following the success of the feasibility study with a

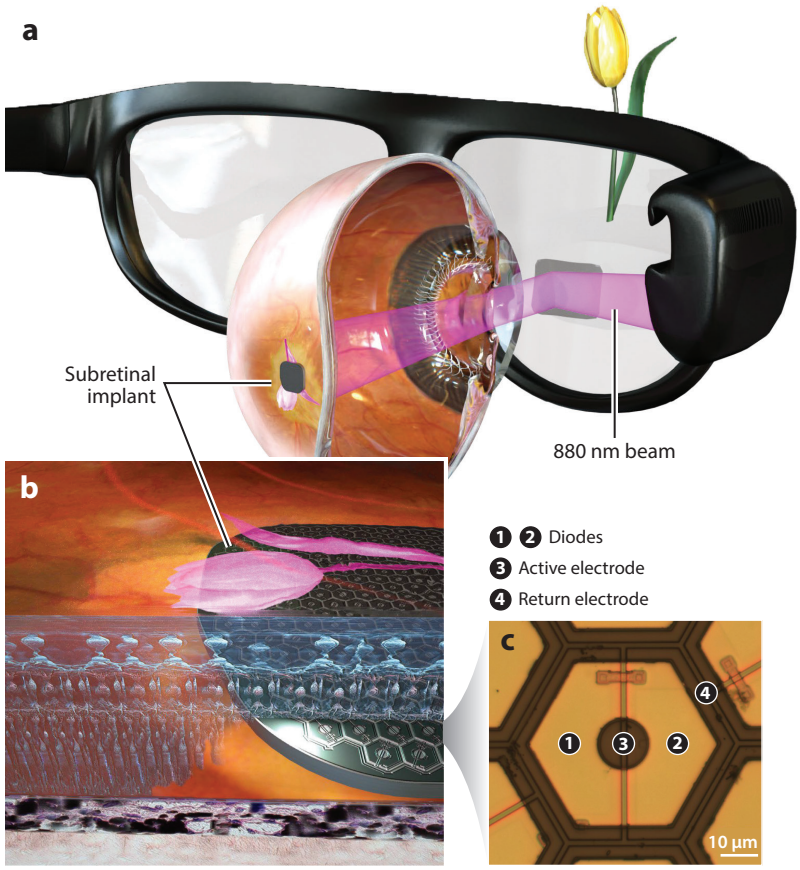

Figure 4

The PRIMA subretinal photovoltaic implant. (*a*) A camera in augmented reality glasses captures the visual scene. Images are then processed and projected into the eye using pulsed near-infrared (880 nm) light. (*b*) The 30 µm thick subretinal implant is composed of photovoltaic pixels, which convert incoming light into electric current to stimulate the nearby inner retinal neurons. (*c*) Close-up of a pixel, which includes two diodes (*1* and *2*) connected in series between the active (*3*) and return (*4*) electrodes. Figure adapted from Palanker et al. (2020).

4-year follow-up (Muqit et al. 2024), a larger study involving 38 patients treated in five European countries was conducted, with results from the first 12-month follow-up presented at the September 2024 Euretina conference in Barcelona (Holz et al. 2024) and announced at a press release by Science Corp. (Science 2024). Using electronic zoom, patients demonstrated a mean improvement of visual acuity of 24 ETDRS letters (4.8 lines) compared to baseline, without a decrease in residual natural acuity.

3.3. Suprachoroidal Prostheses

Suprachoroidal prostheses are placed between the choroid and the sclera, resulting in separation from the retina by several hundred microns. Placement in this location reduces the risks of retinal damage from surgery and improves heat dissipation since blood flow through choroidal vessels can effectively carry away the heat from the chip (Hadjinicolaou et al. 2015, Parver et al. 1983).

However, the increased distance between the electrode and target tissue leads to divergence of electric current, resulting in an elevated stimulation threshold and reduced spatial resolution (Yamauchi et al. 2005). Typically, a return electrode is placed in the anterior part of the eye, such as the cornea or vitreous cavity, to guarantee current flow through the RPE and retina.

A suprachoroidal-transretinal stimulation (STS) system was implanted semichronically in 3 patients with outer retinal degeneration (Fujikado et al. 2016). The implant was positioned in a scleral pocket (6 × 5 mm) formed by cutting a flap in the sclera, and its electronic metal case was located subdermally behind the ears (Morimoto et al. 2011). Forty-nine platinum electrodes of 500 μm diameter formed a 7 × 7 array. About 50% of the electrodes could elicit phosphenes below the threshold (1 mA, 0.4 ms pulses at 20 Hz for 1 s). No serious adverse events emerged during the 12-month study period. Functional testing results were mixed: Patient 3 showed improvement in localizing a square on a screen, following a line while walking, and finding objects on a table (all better with the system on versus off), but patients 1 and 2 were less consistent in these experiments. The implants were removed after 12 months.

Bionic Vision Technologies has tested two generations of suprachoroidal implants in blind subjects. The prototype was implanted in 3 RP patients for a phase I clinical trial. Similar to Alpha-IMS, a percutaneous connector was used for access to the stimulating electrode array. Postsurgical monitoring up to 2 years showed that the device remained functional and stable in the suprachoroidal space with no significant retinal edema or atrophy. Similar to what has been found with epiretinal implants, the threshold for generating perceivable phosphenes increased with larger distance between the electrodes and the retina (de Balthasar et al. 2008). In visual function tests, all 3 patients were able to perform light spot localization with accuracy better than chance level, and the equivalent visual acuity was estimated at 2.62 LogMAR (20/8397) (Ayton et al. 2014).

Based on the safety profiles of the first 3 patients, Bionic Vision Technologies conducted a phase II clinical trial of the second-generation suprachoroidal implant with 44 electrodes in 4 patients with advanced RP with bare light perception only (Petoe et al. 2021). Device implantation was successful, and there were no device-related serious adverse events (**Figure 5**). The macular position of the electrode array was confirmed by optical coherence tomography. Two subjects showed mild postoperative subretinal bleeding, which resolved spontaneously within 2 weeks. Functional testing showed improved object localization in all subjects (with the device on versus off) and improved motion discrimination in 2 of the 4 subjects (also with the device on versus off). All subjects were able to use the device to perform basic mobility tasks. A second report, 2.7 years after implantation, essentially confirmed the interim results (Petoe et al. 2025). Importantly, no device-related serious adverse events were noted. Participants reported on how they used the artificial vision in their daily lives, providing examples such as exploring new environments, detecting people, and safely navigating around obstacles. An independent assessor visited participants in their homes and confirmed the positive effect of the artificial vision on participants' daily lives in their local environments.

4. CHALLENGES AND FUTURE DIRECTIONS

The first two major commercial efforts attempting prosthetic restoration of sight in patients with no light perception due inherited retinal degeneration (i.e., RP) using epiretinal (i.e., ARGUS II) and subretinal (i.e., Alpha-IMS, Alpha-AMS) implants have proven that visual percepts can be elicited electrically in the degenerate retina. However, they failed to reach an acceptable level of performance, and these products were discontinued. The next generation of implants are designed to address their shortcomings. For example, arcuate visual percepts, a major issue resulting from axonal stimulation by epiretinal implants (Grosberg et al. 2017, Nanduri et al. 2012), might be

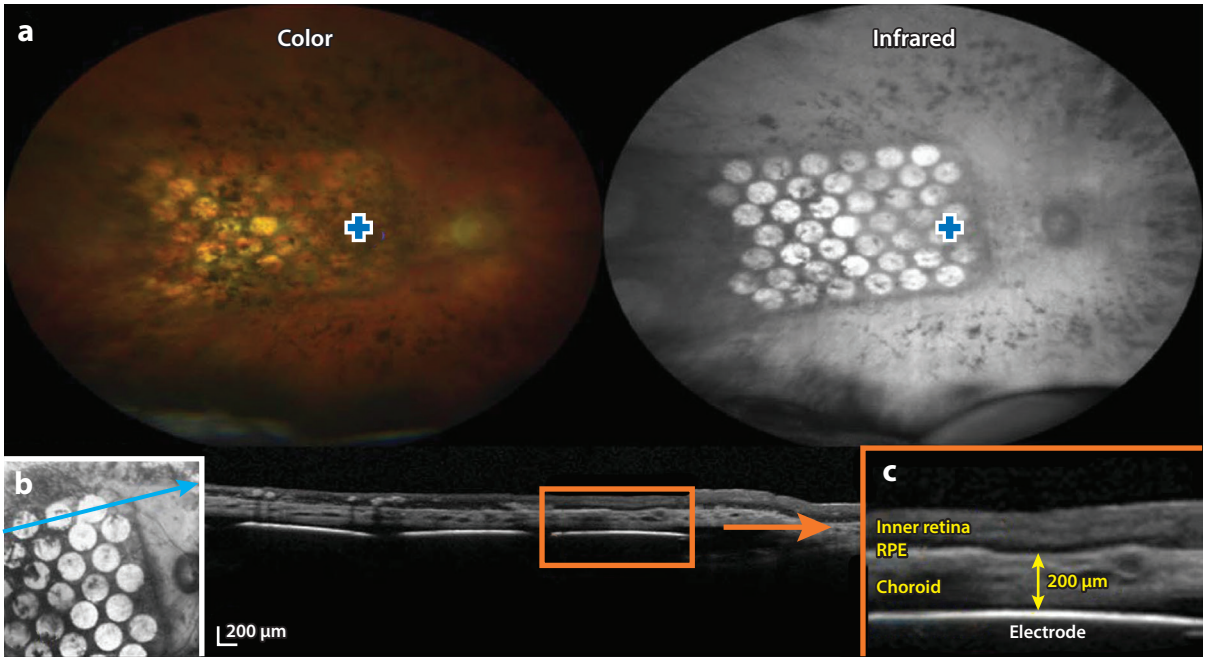

Figure 5

A 44-channel suprachoroidal retinal prosthesis. (*a*) Fundus images of the electrode array at 12 weeks after surgery with RGB (*left*) and infrared (*right*) illumination. Dark blue plus signs mark the fovea. The leading edge of the electrode array is surgically inserted toward the optic disc, with the trailing edge and lead wire (not shown) extending toward the periphery. (*b*) Optical coherence tomography image of the electrode array at 4 weeks after surgery. The light blue arrow indicates the B-scan position through the retina and electrode array. (*c*) Magnified view of the orange box in panel *b*, showing the inner retina, retinal pigment epithelium (RPE), choroid, and suprachoroidal electrode. The yellow arrow shows the electrode-to-retina distance (200 µm). Figure reproduced with permission from Petoe et al. (2021) (CC BY-NC-ND 4.0).

circumvented by using much longer (> 20 ms rather than < 1 ms) pulses to stimulate bipolar rather than ganglion cells (Weitz et al. 2015). Alternatively, with a dense array of epiretinal microelectrodes, only the ones that induce selective activation of local ganglion cells will be used (Grosberg et al. 2017).

Clinical experience with retinal (and cortical) prostheses demonstrated that pattern stimulation does not always result in pattern perception, meaning that perceived shapes may be very different from stimulation patterns. Since the encoding of visual information becomes more and more distributed and specialized as it propagates through the neural network, its replacement with prosthetic stimulation becomes more challenging the further away the target cells are from photoreceptors. In this regard, subretinal stimulation of bipolar cells has better chances of preserving at least some of the retinal code compared to direct stimulation of RGCs. In fact, it has been demonstrated that subretinal stimulation evoked ON and OFF responses with antagonistic center-surround (Ho et al. 2018b), nonlinear summation of bipolar cell subunits in RGCs (Lorach et al. 2015), flicker fusion (Ho et al. 2019, Lorach et al. 2015), and other properties of natural signal processing in the retina. Subretinal photovoltaic stimulation in AMD patients resulted in retinotopically correct visual perception. Moreover, prosthetic central vision being perceived simultaneously with peripheral natural vision, and even merging, indicates that the prosthetic retinal code was sufficiently similar to the natural code. The fact that patients with such implants perceive light stimuli as bright rather than dark percepts suggests that despite

indiscriminate stimulation of ON and OFF bipolar cells, the ON pathway dominates, probably due to asymmetric suppression of the OFF channel in the retinal network (Liang & Freed 2010). Another reason for the dominance of the ON pathway in prosthetic vision could be the fact that the OFF pathway becomes noisy in retinal degeneration, exhibiting a high spontaneous firing rate, while the ON pathway retains low levels of spontaneous activity (Sekirnjak et al. 2011). Therefore, a similar number of elicited spikes corresponds to a much higher signal-to-noise ratio in the ON pathway, while its contribution in the OFF pathway may be negligible.

One issue that might explain the better results with the PRIMA subretinal implant in AMD patients than with the Alpha-AMS implant in RP patients is that in AMD patients, the retinal network is much better preserved due to the relatively small size of the scotoma than in the end-stage RP retina. In addition, local return electrodes in PRIMA provide much better confinement of the electric field around each pixel, thereby improving the selectivity, resolution, and contrast of the stimulation patterns. Finally, shorter disease duration in AMD likely results in less pronounced inner retinal circuitry remodeling as compared to RP. As a result, patients with the PRIMA system demonstrated form prosthetic vision with acuity matching the 100 μm pixel size (20/420) and reaching 20/63 with electronic zoom (Muqit et al. 2024). The next-generation implant with pixel sizes reduced to 20 μm was successfully tested in rats (Wang et al. 2022). If it works as well in clinical settings, it may enable central vision with acuity better than 20/100 without zoom, and up to 20/20 with zoom, which would provide real benefit for many patients with severe visual impairment due to AMD.

An alternative epiretinal approach under development is the artificial retina implant for selective activation of the major classes of RGCs with the appropriate retinal code to restore sight in RP patients despite strong remodeling of their inner retinal network (Shah & Chichilnisky 2020). Currently, this approach is limited to the selective activation of parasol ganglion cells in parafoveal areas, where RGCs are arranged in a monolayer. Parasols have larger somas and lower stimulation thresholds than midget RGCs, making their selective stimulation especially suitable in the raphe area, on the horizontal axis of the retina, where the number of axonal bundles is minimal (Shah et al. 2024). This project faces significant technical challenges, but if successful, it has the potential to properly restore many features of natural vision.

Systems with external image processing capabilities, such as PRIMA or the artificial retina, can benefit from advancements in computer vision, including correction of the gray scale to maximize the dynamic range and contrast sensitivity of prosthetic vision for each patient, as well as enhancements for face representation and other natural scenes (Park et al. 2025). Commercialization of such complex technology as brain–machine interfaces in general and retinal prostheses in particular is another challenge; therefore, these developments typically require a consortium of an academic group performing basic and preclinical studies and a commercial entity for clinical implementation and testing.

SUMMARY POINTS

1. Retinal prostheses aim to restore sight to patients blinded due to loss of photoreceptors by using electrical stimulation of inner retinal neurons.
2. Subretinal implants stimulate second-order neurons, bipolar cells, and rely on transmission of their signals through the retinal neural network to output neurons, ganglion cells, which generate bursts of action potentials propagating via the optic nerve to the brain.

Due to network-mediated stimulation, many features of natural retinal signal processing can be preserved in this approach.

3. Epiretinal implants stimulate primarily ganglion cells and hence encode visual information directly in the spiking patterns. Ideally, the stimulation protocol should match the target cell types (ON, OFF, transient, sustained, etc.).
4. Retinal prostheses have elicited perception of light in patients blinded by inherited retinal degeneration, but so far, they have failed to achieve an acceptable level of performance, and companies have discontinued these products.
5. Recent clinical trials of subretinal photovoltaic arrays in patients blinded by atrophic age-related macular degeneration demonstrated form vision with letter acuity of 20/420, matching the pixel pitch of 100 μm. Using electronic zoom, patients could read and write much smaller fonts, up to 20/100 or even 20/63.

FUTURE DIRECTIONS

1. Preclinical measurements with the next-generation photovoltaic implant with 20 μm pixels reached the 28 μm natural limit of grating acuity in rats. Such implants may provide 20/80 acuity in humans (without zoom), and they are now being transferred to industrial manufacturing and clinical testing.
2. Novel epiretinal systems are being developed for selective activation of specific types of ganglion cells, with appropriate sequences of pulses to replicate the retinal code.
3. Systems with external cameras can benefit from image processing capability to maximize the dynamic range and contrast sensitivity of prosthetic vision in each patient, enhance face representation, and perceive other aspects of natural scenes.

DISCLOSURE STATEMENT

D.P. is a consultant to Science Corp., which commercializes the PRIMA retinal prosthesis, and an author of patents licensed to Science Corp. from Stanford University. J.D.W. had a research relationship with Second Sight Medical Products, which built and sold the Argus II retinal implant. J.-A.S. co-founded Pixium Vision, which has supported the clinical development of PRIMA, and was an unpaid principal investigator on the Second Sight ARGUS II trial.

ACKNOWLEDGMENTS

D.P. has received funding support from the National Institutes of Health (NIH) (R01-EY-027786, R01-EY-035227, and P30-EY026877), the Department of Defense (grant W81XWH-19-1-0738), and the Air Force Office of Scientific Research (grant FA9550-19-1-0402). J.A.S. has received funding support through an unrestricted grant from Research to Prevent Blindness and an NIH Core P30 Grant to the University of Pittsburgh.

LITERATURE CITED

Ahuja AK, Dorn JD, Caspi A, McMahon MJ, Dagnelie G, et al. 2011. Blind subjects implanted with the Argus II retinal prosthesis are able to improve performance in a spatial-motor task. *Br. J. Ophthalmol.* 95(4):539–43

Arens-Arad T, Farah N, Lender R, Moshkovitz A, Flores T, et al. 2020. Cortical interactions between prosthetic and natural vision. *Curr. Biol.* 30(1):176–82.e2

Ayton LN, Blamey PJ, Guymer RH, Luu CD, Nayagam DAX, et al. 2014. First-in-human trial of a novel suprachoroidal retinal prosthesis. *PLOS ONE* 9(12):e115239

Behrend MR, Ahuja AK, Humayun MS, Chow RH, Weilan JD. 2011. Resolution of the epiretinal prosthesis is not limited by electrode size. *IEEE Trans. Neural Syst. Rehabil. Eng.* 19(4):436–42

Berson EL. 2007. Long-term visual prognoses in patients with retinitis pigmentosa: the Ludwig von Sallmann lecture. *Exp. Eye Res.* 85(1):7–14

Bhuckory MB, Monkongpitukkul N, Shin A, Kochnev Goldstein A, Jensen N, et al. 2025. Enhancing prosthetic vision by upgrade of a subretinal photovoltaic implant in situ. *Nat. Commun.* 16:2820

Boinagrov D, Loudin J, Palanker D. 2010. Strength-duration relationship for extracellular neural stimulation: numerical and analytical models. *J. Neurophysiol.* 104(4):2236–48

Boinagrov D, Pangratz-Fuehrer S, Goetz G, Palanker D. 2014. Selectivity of direct and network-mediated stimulation of the retinal ganglion cells with epi-, sub- and intraretinal electrodes. *J. Neural Eng.* 11(2):026008

Briggman KL, Helmstaedter M, Denk W. 2011. Wiring specificity in the direction-selectivity circuit of the retina. *Nature* 471(7337):183–88

Britten KH, Shadlen MN, Newsome WT, Movshon JA. 1992. The analysis of visual motion: a comparison of neuronal and psychophysical performance. *J. Neurosci.* 12(12):4745–65

Butterwick A, Vankov A, Huie P, Freyvert Y, Palanker D. 2007. Tissue damage by pulsed electrical stimulation. *IEEE Trans. Biomed. Eng.* 54(12):2261–67

Caspi A, Roy A, Wuyyuru V, Rosendall PE, Harper JW, et al. 2018. Eye movement control in the Argus II retinal-prosthesis enables reduced head movement and better localization precision. *Investig. Ophthalmol. Vis. Sci.* 59(2):792–802

Cho A, Ratliff C, Sampath A, Weiland J. 2016. Changes in ganglion cell physiology during retinal degeneration influence excitability by prosthetic electrodes. *J. Neural Eng.* 13(2):025001

Chow AY, Bittner AK, Pardue MT. 2010. The artificial silicon retina in retinitis pigmentosa patients (an American Ophthalmological Association thesis). *Trans. Am. Ophthalmol. Soc.* 108:120–54

Chow AY, Chow VY, Packo KH, Pollack JS, Peyman GA, Schuchard R. 2004. The artificial silicon retina microchip for the treatment of vision loss from retinitis pigmentosa. *Arch. Ophthalmol.* 122(4):460–69

Cogan SF. 2008. Neural stimulation and recording electrodes. *Annu. Rev. Biomed. Eng.* 10:275–309

daCruz L, Coley B, Christopher P, Merlini F, Wuyyuru V, et al. 2010. Patients blinded by outer retinal dystrophies are able to identify letters using the Argus TM II retinal prosthesis system. *Investig. Ophthalmol. Vis. Sci.* 51(13):2023

Dandona L, Dandona R. 2006. Revision of visual impairment definitions in the International Statistical Classification of Diseases. *BMC Med.* 4:7

Daschner R, Rothermel A, Rudorf R, Rudorf S, Stett A. 2018. Functionality and performance of the subretinal implant chip Alpha AMS. *Sens. Mater.* 30(2):179–92

de Balthasar C, Patel S, Roy A, Freda R, Greenwald S, et al. 2008. Factors affecting perceptual thresholds in epiretinal prostheses. *Investig. Ophthalmol. Vis. Sci.* 49(6):2303–14

Delyfer M-N, Gaucher D, Mohand-Saïd S, Barale P-O, Rezaigua-Studer F, et al. 2021. Improved performance and safety from Argus II retinal prosthesis post-approval study in France. *Acta Ophthalmol.* 99(7):e1212–21

EDPRG (Eye Diseases Prevalence Research Group). 2004. Prevalence of age-related macular degeneration in the United States. *Arch. Ophthalmol.* 122(4):564–72

Fried SI, Hsueh HA, Werblin FS. 2006. A method for generating precise temporal patterns of retinal spiking using prosthetic stimulation. *J. Neurophysiol.* 95(2):970–78

Fujikado T, Kamei M, Sakaguchi H, Kanda H, Endo T, et al. 2016. One-year outcome of 49-channel suprachoroidal–transretinal stimulation prosthesis in patients with advanced retinitis pigmentosa. *Investig. Ophthalmol. Vis. Sci.* 57(14):6147–57

Fujikado T, Kamei M, Sakaguchi H, Kanda H, Morimoto T, et al. 2011. Testing of semichronically implanted retinal prosthesis by suprachoroidal-transretinal stimulation in patients with retinitis pigmentosa. *Investig. Ophthalmol. Vis. Sci.* 52(7):4726–33

Geruschat DR, Richards TP, Arditi A, da Cruz L, Dagnelie G, et al. 2016. An analysis of observer-rated functional vision in patients implanted with the Argus II Retinal Prosthesis System at three years. *Clin. Exp. Optom.* 99(3):227–32

Ghezzi D, Antognazza MR, Maccarone R, Bellani S, Lanzarini E, et al. 2013. A polymer optoelectronic interface restores light sensitivity in blind rat retinas. *Nat. Photonics* 7(5):400–6

Greschner M, Field GD, Li PH, Schiff ML, Gauthier JL, et al. 2014. A polyaxonal amacrine cell population in the primate retina. *J. Neurosci.* 34(10):3597–606

Grosberg LE, Ganesan K, Goetz GA, Madugula SS, Bhaskhar N, et al. 2017. Activation of ganglion cells and axon bundles using epiretinal electrical stimulation. *J. Neurophysiol.* 118(3):1457–71

Grover S, Fishman GA, Anderson RJ, Tozatti MS, Heckenlively JR, et al. 1999. Visual acuity impairment in patients with retinitis pigmentosa at age 45 years or older. *Ophthalmology* 106(9):1780–85

Ha S, Khraiche ML, Akinin A, Jing Y, Damle S, et al. 2016. Towards high-resolution retinal prostheses with direct optical addressing and inductive telemetry. *J. Neural Eng.* 13(5):056008

Hadjinicolaou AE, Meffin H, Maturana MI, Cloherty SL, Ibbotson MR. 2015. Prosthetic vision: devices, patient outcomes and retinal research. *Clin. Exp. Optom.* 98(5):395–410

Haim M. 2002. The epidemiology of retinitis pigmentosa in Denmark. *Acta Ophthalmol. Scand.* 80:(s233):1–34

Ho AC, Humayun MS, Dorn JD, da Cruz L, Dagnelie G, et al. 2015. Long-term results from an epiretinal prosthesis to restore sight to the blind. *Ophthalmology* 122(8):1547–54

Ho E, Lei X, Flores T, Lorach H, Huang T, et al. 2019. Characteristics of prosthetic vision in rats with subretinal flat and pillar electrode arrays. *J. Neural Eng.* 16(6):066027

Ho E, Lorach H, Goetz G, Laszlo F, Lei X, et al. 2018a. Temporal structure in spiking patterns of ganglion cells defines perceptual thresholds in rodents with subretinal prosthesis. *Sci. Rep.* 8(1):3145

Ho E, Smith R, Goetz G, Lei X, Galambos L, et al. 2018b. Spatiotemporal characteristics of retinal response to network-mediated photovoltaic stimulation. *J. Neurophysiol.* 119(2):389–400

Holz FG, Le Mer Y, Muqit MMK, Olmos de Koo L, Sahel J. 2024. 12 months interim safety results of the pivotal study of the PRIMA Retinal implant system in patients with geographic atrophy: the PRIMAvera clinical trial. Paper presented at the 24th Euretina Congress

Hornig R, Dapper M, Joliff EL, Hill R. 2017. Pixium vision: first clinical results and innovative developments. In *Artificial Vision: A Clinical Guide*, ed. VP Gabel. Springer International Publishing

Humayun MS, Dorn JD, da Cruz L, Dagnelie G, Sahel J-A, et al. 2012. Interim results from the international trial of Second Sight's visual prosthesis. *Ophthalmology* 119(4):779–88

Humayun MS, Prince M, de Juan E Jr., Barron Y, Moskowitz M, Klock IB, Milam AH. 1999. Morphometric analysis of the extramacular retina from postmortem eyes with retinitis pigmentosa. *Investig. Ophthalmol. Vis. Sci.* 40(1):143–48

Humayun MS, Weiland JD, Fujii GY, Greenberg R, Williamson R, et al. 2003. Visual perception in a blind subject with a chronic microelectronic retinal prosthesis. *Vis. Res.* 43(24):2573–81

ISO (International Organization for Standardization). 2014. *Implants for surgery—active implantable medical devices. Part 1: General requirements for safety, marking and for information to be provided by the manufacturer*. ISO 14708-1:2014, ISO. **https://www.iso.org/standard/52804.html**

Jensen RJ, Rizzo JF III. 2006. Thresholds for activation of rabbit retinal ganglion cells with a subretinal electrode. *Exp. Eye Res.* 83(2):367–73

Jensen RJ, Ziv OR, Rizzo JF III. 2005. Thresholds for activation of rabbit retinal ganglion cells with relatively large, extracellular microelectrodes. *Investig. Ophthalmol. Vis. Sci.* 46(4):1486–96

Jones BW, Marc RE. 2005. Retinal remodeling during retinal degeneration. *Exp. Eye Res.* 81(2):123–37

Kim SY, Sadda S, Pearlman J, Humayun MS, de Juan E Jr., Melia BM, Green WR. 2002. Morphometric analysis of the macula in eyes with disciform age-related macular degeneration. *Retina* 22(4):471–7

Knutson JS, Naples GG, Peckham PH, Keith MW. 2002. Electrode fracture rates and occurrences of infection and granuloma associated with percutaneous intramuscular electrodes in upper-limb functional electrical stimulation applications. *J. Rehabil. Res. Dev.* 39(6):671–83

Liang Z, Freed MA. 2010. The ON pathway rectifies the OFF pathway of the mammalian retina. *J. Neurosci.* 30(16):5533–43

Lorach H, Goetz G, Smith R, Lei X, Mandel Y, et al. 2015. Photovoltaic restoration of sight with high visual acuity. *Nat. Med.* 21(5):476–82

Loudin JD, Simanovskii DM, Vijayraghavan K, Sramek CK, Butterwick AF, et al. 2007. Optoelectronic retinal prosthesis: system design and performance. *J. Neural Eng.* 4(1):S72–84

Marc RE, Jones BW. 2003. Retinal remodeling in inherited photoreceptor degenerations. *Mol. Neurobiol.* 28(2):139–47

Marc RE, Jones BW, Watt CB, Strettoi E. 2003. Neural remodeling in retinal degeneration. *Prog. Retin. Eye Res.* 22(5):607–55

Margolis DJ, Newkirk G, Euler T, Detwiler PB. 2008. Functional stability of retinal ganglion cells after degeneration-induced changes in synaptic input. *J. Neurosci.* 28(25):6526–36

Masland RH. 2001. The fundamental plan of the retina. *Nat. Neurosci.* 4(9):877–86

Mathieson K, Loudin J, Goetz G, Huie P, Wang L, et al. 2012. Photovoltaic retinal prosthesis with high pixel density. *Nat. Photonics* 6(6):391–97

Mazzoni F, Novelli E, Strettoi E. 2008. Retinal ganglion cells survive and maintain normal dendritic morphology in a mouse model of inherited photoreceptor degeneration. *J. Neurosci.* 28(52):14282–92

McCreery DB, Agnew WF, Yuen TGH, Bullara L. 1990. Charge-density and charge per phase as cofactors in neural injury induced by electrical-stimulation. *IEEE Trans. Biomed. Eng.* 37(10):996–1001

Menzler J, Zeck G. 2011. Network oscillations in rod-degenerated mouse retinas. *J. Neurosci.* 31(6):2280–91

Merigan WH, Maunsell JHR. 1993. How parallel are the primate visual pathways? *Annu. Rev. Neurosci.* 16:369–402

Merrill DR, Bikson M, Jefferys JGR. 2005. Electrical stimulation of excitable tissue: design of efficacious and safe protocols. *J. Neurosci. Methods* 141(2):171–98

Morimoto T, Kamei M, Nishida K, Sakaguchi H, Kanda H, et al. 2011. Chronic implantation of newly developed suprachoroidal-transretinal stimulation prosthesis in dogs. *Investig. Ophthalmol. Vis. Sci.* 52(9):6785–92

Muqit MMK, Le Mer Y, Olmos de Koo L, Holz FG, Sahel JA, Palanker D. 2024. Prosthetic visual acuity with the PRIMA subretinal microchip in patients with atrophic age-related macular degeneration at 4 years follow-up. *Ophthalmol. Sci.* 4(5):100510

Nanduri D, Fine I, Horsager A, Boynton GM, Humayun MS, et al. 2012. Frequency and amplitude modulation have different effects on the percepts elicited by retinal stimulation. *Investig. Ophthalmol. Vis. Sci.* 53(1):205–14

Naumann J. 2012. *Search for Paradise: A Patient's Account of the Artificial Vision Experiment*. Xlibris

Neumann E. 1992. Membrane electroporation and direct gene-transfer. *Bioelectrochem. Bioenerget.* 28(1–2):247–67

Osepchuck JM, ed. 1983. *Biological Effects of Electromagnetic Radiation*. IEEE Press

Palanker D, Blumenkranz MS, Weiter JJ. 2005a. Retinal laser therapy: biophysical basis and applications. In *Retina*, ed. SJ Ryan. Mosby. 4th ed.

Palanker D, Le Mer Y, Mohand-Said S, Muqit M, Sahel JA. 2020. Photovoltaic restoration of central vision in atrophic age-related macular degeneration. *Ophthalmology* 127(8):1097–104

Palanker D, Le Mer Y, Mohand-Said S, Sahel JA. 2022. Simultaneous perception of prosthetic and natural vision in AMD patients. *Nat. Commun.* 13(1):513

Palanker D, Vankov A, Huie P, Baccus S. 2005b. Design of a high-resolution optoelectronic retinal prosthesis. *J. Neural Eng.* 2(1):S105–20

Park J, Kochnev Goldstein A, Zhuo Y, Jensen N, Palanker D. 2025. Simulation of prosthetic vision with PRIMA system and enhancement of face representation. Preprint, arXiv:2503.11677v2 [cs.HC]

Parver LM, Auker CR, Carpenter DO. 1983. Choroidal blood flow. III. Reflexive control in human eyes. *Arch. Ophthalmol.* 101(10):1604–6

Petoe MA, Abbott CJ, Titchener SA, Kolic M, Kentler WG, et al. 2025. A second-generation (44-channel) suprachoroidal retinal prosthesis: a single-arm clinical trial of feasibility. *Ophthalmol. Sci.* 5(1):100525

Petoe MA, Titchener SA, Kolic M, Kentler WG, Abbott CJ, et al. 2021. A second-generation (44-channel) suprachoroidal retinal prosthesis: interim clinical trial results. *Transl. Vis. Sci. Technol.* 10(10):12

Rizzo S, Cinelli L, Finocchio L, Tartaro R, Santoro F, Gregori NZ. 2019. Assessment of postoperative morphologic retinal changes by optical coherence tomography in recipients of an electronic retinal prosthesis implant. *JAMA Ophthalmol.* 137:272–78

Robblee LS, Rose TL. 1990. Electrochemical guidelines for selection of protocols and electrode materials for neural stimulation. In *Neural Prostheses: Fundamental Studies*, ed. WF Agnew, DB McCreery. Prentice Hall

Rudnicka AR, Jarrar Z, Wormald R, Cook DG, Fletcher A, Owen CG. 2012. Age and gender variations in age-related macular degeneration prevalence in populations of European ancestry: a meta-analysis. *Ophthalmology* 119(3):571–80

Salzman CD, Britten KH, Newsome WT. 1990. Cortical microstimulation influences perceptual judgements of motion direction. *Nature* 346(6280):174–77

Science. 2024. Science announces positive preliminary results for vision restoration in pivotal clinical trial. Science. **https://science.xyz/news/primavera-trial-preliminary-results/**

Sekirnjak C, Jepson LH, Hottowy P, Sher A, Dabrowski W, et al. 2011. Changes in physiological properties of rat ganglion cells during retinal degeneration. *J. Neurophysiol.* 105(5):2560–71

Shah NP, Chichilnisky EJ. 2020. Computational challenges and opportunities for a bi-directional artificial retina. *J. Neural Eng.* 17(5):055002

Shah NP, Phillips AJ, Madugula S, Lotlikar A, Gogliettino AR, et al. 2024. Precise control of neural activity using dynamically optimized electrical stimulation. *eLife* 13:e83424

Smith W, Assink J, Klein R, Mitchell P, Klaver CC, et al. 2001. Risk factors for age-related macular degeneration: pooled findings from three continents. *Ophthalmology* 108(4):697–704

Stingl K, Bartz-Schmidt KU, Besch D, Chee CK, Cottriall CL, et al. 2015. Subretinal visual implant Alpha IMS–clinical trial interim report. *Vis. Res.* 111:149–60

Stingl K, Schippert R, Bartz-Schmidt KU, Besch D, Cottriall CL, et al. 2017. Interim results of a multicenter trial with the new electronic subretinal implant Alpha AMS in 15 patients blind from inherited retinal degenerations. *Front. Neurosci.* 11:445

Tochitsky I, Polosukhina A, Degtyar VE, Gallerani N, Smith CM, et al. 2014. Restoring visual function to blind mice with a photoswitch that exploits electrophysiological remodeling of retinal ganglion cells. *Neuron* 81(4):800–13

Wandell B. 1995. *Foundations of Vision*. Sinauer Associates

Wang B-Y, Chen ZC, Bhuckory M, Huang T, Shin A, et al. 2022. Electronic photoreceptors enable prosthetic visual acuity matching the natural resolution in rats. *Nat. Commun.* 13(1):6627

Wang G, Liu WT, Sivaprakasam M, Kendir GA. 2005. Design and analysis of an adaptive transcutaneous power telemetry for biomedical implants. *IEEE Trans. Circuits Syst. I Regul. Pap.* 52(10):2109–17

Wassle H. 2004. Parallel processing in the mammalian retina. *Nat. Rev. Neurosci.* 5(10):747–57

Weitz AC, Nanduri D, Behrend MR, Gonzalez-Calle A, Greenberg RJ, et al. 2015. Improving the spatial resolution of epiretinal implants by increasing stimulus pulse duration. *Sci. Transl. Med.* 7(318):318ra203

Werginz P, Benav H, Zrenner E, Rattay F. 2015. Modeling the response of ON and OFF retinal bipolar cells during electric stimulation. *Vis. Res.* 111(Pt. B):170–81

Wilke R, Gabel V-P, Sachs H, Bartz Schmidt K-U, Gekeler F, et al. 2011. Spatial resolution and perception of patterns mediated by a subretinal 16-electrode array in patients blinded by hereditary retinal dystrophies. *Investig. Ophthalmol. Vis. Sci.* 52(8):5995–6003

Wong WL, Su X, Li X, Cheung CMG, Klein R, et al. 2014. Global prevalence of age-related macular degeneration and disease burden projection for 2020 and 2040: a systematic review and meta-analysis. *Lancet Glob. Health* 2(2):e106–16

Woodburn KW, Engelman CJ, Blumenkranz MS. 2002. Photodynamic therapy for choroidal neovascularization: a review. *Retina* 22(4):391–405

Xu H, Zhong X, Pang C, Zou J, Chen W, et al. 2021. First human results with the 256 channel intelligent micro implant eye (IMIE 256). *Trans. Vis. Sci. Technol.* 10(10):14

Yamauchi Y, Franco LM, Jackson DJ, Naber JF, Ziv RO, et al. 2005. Comparison of electrically evoked cortical potential thresholds generated with subretinal or suprachoroidal placement of a microelectrode array in the rabbit. *J. Neural Eng.* 2(1):S48–56

Yanai D, Weiland JD, Mahadevappa M, Greenberg RJ, Fine I, Humayun MS. 2007. Visual performance using a retinal prosthesis in three subjects with retinitis pigmentosa. *Am. J. Ophthalmol.* 143(5):820–27

Yanovitch L, Raz-Prag D, Hanein Y. 2022. A new high-resolution three-dimensional retinal implant: *system design and preliminary human results*. Preprint, bioRxiv. **https://www.biorxiv.org/content/10.1101/2022.09.14.507901v1.abstract**

Yue L, Falabella P, Christopher P, Wuyyuru V, Dorn J, et al. 2015. Ten-year follow-up of a blind patient chronically implanted with epiretinal prosthesis Argus I. *Ophthalmology* 122(12):2545–52.e1

Zrenner E, Bartz-Schmidt KU, Benav H, Besch D, Bruckmann A, et al. 2011. Subretinal electronic chips allow blind patients to read letters and combine them to words. *Proc. Biol. Sci.* 278(1711):1489–97